Characterization of Epoxy Hybrid Composites Filled with Cellulose Fibers and Nano-SiC

H. Alamri, I. M. Low

Department of Imaging and Applied Physics, Curtin University of Technology, GPO Box U1987, Perth, WA 6845, Australia

Received 14 October 2011; accepted 12 January 2012
DOI 10.1002/app.36815
Published online in Wiley Online Library (wileyonlinelibrary.com).

ABSTRACT: Three different approaches have been applied and investigated to enhance the thermal and mechanical properties of epoxy resin. Epoxy system reinforced with either recycled cellulose fibers (RCF) or nanosilicon carbide (n-SiC) particles as well as with both RCF and n-SiC has been fabricated and investigated. The effect of RCF/n-SiC dispersion on the mechanical and thermal properties of these composites has been characterized. The fracture surface morphology and toughness mechanisms were investigated by scanning electron microscopy. The dispersion of n-SiC particles into epoxy nanocomposites was studied by synchrotron radiation diffraction and transmission electron microscopy. Results indicated that mechanical properties increased as a result of the addition of n-SiC. The presence of RCF layers significantly increased the mechanical properties of RCF/epoxy composites when compared with neat epoxy and its nanocomposites. The influence of the addition of n-SiC to RCF/epoxy composites in mechanical properties was found to be positive in toughness properties. At high temperatures, thermal stability of neat epoxy increased due to the presence of either n-SiC particles or RCF layers. However, the presence of RCF accelerated the thermal degradation of neat epoxy as well as the addition of n-SiC to RCF/epoxy samples increased the rate of the major thermal degradation. © 2012 Wiley Periodicals, Inc. J Appl Polym Sci 000: 000–000, 2012

Key words: recycled cellulose fibers; silicon carbide nanoparticles; nanocomposites; mechanical properties; thermal properties

INTRODUCTION

Epoxy is considered to be one of the important matrices used for fiber-reinforced polymer due to its unique properties of relatively high strength, high modulus, low shrinkage, and excellent chemical and heat resistance.[1,2] It has been widely used in manufacturing applications, such as adhesives, coatings, electronics, and aerospace structures. However, majority of cured epoxy systems show low impact strength, poor resistance to crack propagation and initiation, and low fracture toughness.[1,2] The high cost and brittleness of epoxy resins are the main draw backs to its industrial use.[3] Two different approaches have recently been reported in the literature to substantially enhance the properties and reduce the cost of the composite compared to that for the neat epoxy resin.

The first approach dealt with the use of natural cellulose fibers such as flax, hemp, sisal, kenaf, and jute, as reinforcements in the polymeric matrices for making low cost engineering materials. Cellulose fiber reinforced polymers have gained a great attention in engineering applications due to their tremendous properties, which include low density, low cost, renewability and recyclability as well as excellent mechanical characteristics such as flexibility, high toughness, specific strength, and high specific modulus.[4–6] Moreover, there is much pressure on manufacturing industries especially packaging, construction and automotive industries to utilize new materials in substituting the nonrenewable reinforcing materials for instance glass fiber emerging from consumers and new environmental legislation due to increased sensitivity on environmental pollution.[4] Natural fibers have been preferred as they are considered to be environmental friendly (green composites), thus being utilized as a substitute to traditional fiber reinforced petroleum-based composites including aramid fibers, carbon, and glass fibers.[5,6] However, plant fiber reinforced polymeric composites have several drawbacks which include fiber high moisture absorption, incompatibility with some of the polymeric matrices, and poor wettability.[4,7] There is significant amount of work can be found in the literature on the effects of additional cellulose fibers on mechanical, physical, and thermal properties of the polymer systems.[3,7–13]

The second approach dealt with the use of nanosized inorganic particles as modifiers for brittle polymers. In recent years, polymer-clay nanocomposites (PCNs) have drawn much attention due to their excellent characteristics such as improvement in physical (shrinkage,

Correspondence to: I. M. Low (j.low@curtin.edu.au).

optical, dielectrics, and permeability), thermal (i.e. thermal expansion coefficient, flammability, decomposition, and thermal stability), and mechanical (i.e. toughness, strength, and modulus) properties.[14–16] Many researchers have studied nanoclay addition effect on thermal, mechanical, and physical properties of polymeric composites since the demonstration of vast improvements in mechanical and physical properties by the pioneering work of researchers on nylon-6/clay nanocomposites at Toyota.[17–25]

Silicon carbide particles are very attractive ceramic material that can be used as filler in different polymer matrices due to the unique properties including high thermal conductivity, low thermal expansion coupled with high strength, high hardness, and high elastic modulus.[26] Silicon carbide (SiC) is rigid crystalline material that compound of silicon and carbon that has been used in grinding abrasive products including wheels for over a period of 100 years.[26] Currently, the material has been developed to a point that it has very good mechanical properties as a high-quality grade ceramic used in numerous high-performance applications.[26] Therefore, ceramic-filled polymer composites have been the subject of extensive research in the last two decades.[27–32] Blackman et al.[27] and Johnsen et al.[28] both reported a significant improvement in fracture toughness for epoxy nanocomposites due to the addition of nanosilica. Zhao et al.[29] on the other hand used nanoalumina particles to toughen epoxy resin. However, no improvement was reported in fracture toughness due to the addition of nanoalumina. Chen et al.[30] reported an increment by 30% in fracture toughness of silica-epoxy nanocomposites compared to neat epoxy. Chatterjee et al.[31] carried out the mechanical and thermal properties of TiO_2/epoxy nanocomposites prepared by ultrasonic mixing process. Authors reported an enhancement in thermal stability, glass transition temperature, tensile and flexural modulus due to the presence of nanosilica particles. However, no improvement was reported in tensile and flexural strength. Ma et al.[32] investigated the effect of silica nanoparticles on the mechanical properties of two types of epoxy systems. It was found that the presence of nanosilica increased Young's modulus, tensile strength, fracture toughness, and impact toughness for both epoxy systems. An increase in nanosilica subsequently resulted to increased mechanical properties.

In this article, the focus is on generating different modes of toughening and strengthening by describing an alternative approach in designing eco-nanocomposites in which elements are tailored with fine dispersions of recycled cellulose fibers (RCF) and nanosilicon carbide (n-SiC). The main idea is to produce an outer epoxy layer dispersed with nanosized SiC for wear resistance and hardness, and with under layers RCF/SiC reinforced epoxy for damage tolerance and toughness. The effect of RCF/n-SiC dispersion on the microstructure, mechanical, and thermal properties have been characterized and discussed in terms of synchrotron radiation diffraction (SRD), transmission electron microscopy (TEM), scanning electron microscopy (SEM), flexural strength and modulus, fracture toughness, impact strength, impact toughness, and thermogravimetric analysis (TGA).

TABLE I
Physical Properties of n-SiC Powder

Properties	Values
Color	Light grey
Particle size	<100 nm
Surface area	70–90 m^2/g
Bulk density	0.069 g/cm^3
Density	3.22 g/cm^3 at 25°C

MATERIALS AND FABRICATION

Materials

RCF paper and nanosilicon carbide (n-SiC) particles were used as reinforcements for the fabrication of epoxy-matrix composites. The RCF paper with grade 200 GSM and 200 μm thickness was supplied by Fuji Xerox Australia, Belmont WA, Australia. n-SiC particles were provided by Sigma-Aldrich LLC, USA. The physical properties of n-SiC particles are outlined in Table I.[33] Finally, general purpose low viscosity epoxy resin (FR-251) and epoxy hardener were supplied by Fiberglass and Aesin Sales, WA, Perth, Australia.

Sample fabrication

Nanocomposites

The n-SiC/epoxy nanocomposites were prepared by mixing the epoxy resin with three different weight percentages (1, 3, and 5%) of n-SiC particles using high speed mechanical mixer for 10 min with a rotation speed of 1200 rpm. After that, a hardener was added to the mixture and then stirred slowly to minimise the formation of air bubbles within the sample. The final mixture was poured into silicon moulds and left for 24 h at room temperature for curing purpose. Pure epoxy (PE) sample was made as a control.

RCF reinforced nanocomposites

In this section, the epoxy system and the nanocomposites dispersed with n-SiC particles were used as the matrix material. RCF sheets were first dried for 60 min at 70°C. After that, RCFs sheets were fully-soaked into a mixture of epoxy/n-SiC until they became entirely wetted by the mixture, before they were laid down in a closed silicone mould under 8.2 kPa compressive pressure and left 24 h for curing at room temperature. The same processing procedure

TABLE II
Compositions of Synthesized n-SiC/Epoxy and RCF-Epoxy/n-SiC Nanocomposites

n-SiC/epoxy samples	n-SiC (wt %)	RCF/SiC/epoxy samples	n-SiC (wt %)
Pure epoxy (PE)	0	PE/RCF	0
PE/SiC1	1	PE/RCF/ SiC1	1
PE/SiC3	3	PE/RCF/ SiC3	3
PE/SiC5	5	PE/RCF/ SiC5	5

was used to prepare RCF/epoxy ecocomposites without the addition of n-SiC. The amount of RCF in the final products was about 48 wt %. All the samples made are summarized in Table II.

Synchrotron radiation diffraction

SRD measurement was carried out on the powder diffraction beamline at the Australian Synchrotron. The diffraction patterns of each sample were collected using a beam of wavelength 1.377 Á in the two-theta range of 2–82°.

Transmission electron microscopy

Ultra-thin sections (~ 80 nm) of samples were prepared using an ultramicrotome (Leica microsystem) and were recovered on a copper grid. Transmission electron microscopy imaging was done using a Titan Cryotwin (FEI Company) operating at 300 kV equipped with a 4 k × 4 k CCD camera (Gatan). TEM was carried out at King Abdullah University of Science and Technology (KAUST), Saudi Arabia.

Scanning electron microscopy

Scanning electron microscope (Zeiss Evo 40XVP) was used to investigate the microstructures and the fracture surfaces of composites. Samples were coated with a thin layer of gold to prevent charging before the observation by SEM.

Thermogravimetric analysis

The thermal stability of samples was studied by TGA and differential thermogravimetry (DTG). A Mettler Toledo TGA/DSC star system analyzer was used for all these measurements. Samples with ~ 10 mg were placed in a platinum can and tests were carried out in nitrogen atmosphere with a heating rate of 10°C/min from 35 to 800°C.

Measurements of mechanical properties

Three-point bend tests

Rectangular bars with dimensions 60 × 10 × 6 mm^3 were cut for three-point bend tests to measure flexural strength, flexural modulus, and fracture toughness. The three-point bend tests were performed using a LLOYD material testing machines—Twin Column Bench Mounted (5–50 kN). The support span used was 40 mm with a displacement rate of 1.0 mm/min. Five specimens of each composition were tested to evaluate the mechanical tests. The flexural strength was evaluated using the following equation:

$$\sigma_F = \frac{3}{2}\frac{p_m S}{WD^2} \tag{1}$$

where P_m is the maximum load at crack extension, S is the span of the sample, D is the specimen thickness, and W is the specimen width. Values of the flexural modulus were computed using the initial slope of the load–displacement curve, $\Delta P/\Delta X$, using the following formula:

$$E_F = \frac{S^3}{4WD^3}\left(\frac{\Delta P}{\Delta X}\right) \tag{2}$$

In order to determine the fracture toughness, a sharp razor blade was used to initiate a sharp crack in the samples. The ratio of crack length to width (a/w) was about (0.4). The fracture toughness was calculated using the following eq. (5):

$$K_{\mathrm{IC}} = \frac{p_m S}{WD^{2/3}} f\left(\frac{a}{w}\right) \tag{3}$$

where a is the crack length and $f(a/w)$ is the polynomial geometrical correction factor given as:

$$f\left(\frac{a}{W}\right) = \frac{3(a/W)^{1/2}[1.99 - (a/W)(1 - a/W) \times (2.15 - 3.93a/W + 2.7a^2/W^2)]}{2(1 + 2a/W)(1 - a/W)^{2/3}} \tag{4}$$

Charpy impact test

Similar rectangular bars were cut for Zwick Charpy impact testing to evaluate the impact strength and impact toughness. A pendulum hammer with 1.0 J was used during the test to break the samples. Unnotched samples were used to compute the impact strength using the following formula:

$$\sigma_I = \frac{E}{A} \tag{5}$$

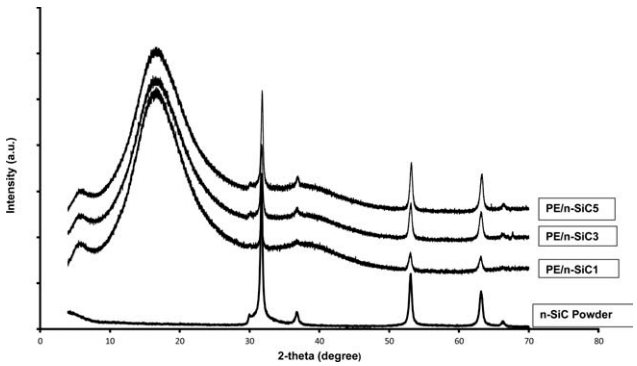

Figure 1 Synchrotron radiation diffraction patterns of n-SiC powder and epoxy/n-SiC nanocomposites.

where E is the impact energy to break a sample with a ligament of area A.

Samples of various notch lengths were used to determine the impact toughness of composites. In order to measure the impact toughness, the value of the critical strain energy release rate (G_{IC}) was evaluated as the slope of the fracture energy (U) versus the energy calibration factor (φ) as shown in the following equation:[5]

$$U = G_{IC}\, WD\phi + U_o \tag{6}$$

where U_o is the kinetic energy, W is the specimen width, and D is the specimen thickness.

RESULTS AND DISCUSSION

Nanocomposites characterization

Synchrotron radiation diffraction

The SRD diffractograms for epoxy/n-SiC nanocomposites and n-SiC powder are shown in Figure 1. The n-SiC patterns show crystalline pattern structure with five sharp peaks in the range of $2\theta = 30$–70°. It also can be seen from Figure 1 that epoxy shows an amorphous structure without distinct repeating unit. The addition of n-SiC particles to epoxy matrix clearly increased the crystallinity of the epoxy/n-SiC composites due to the presence of sharp narrow diffraction peaks. It also can be seen that the highest of the diffraction peaks of n-SiC increased as nanofiller content increased in the epoxy/n-SiC composites.

Transmission electron microscopy

TEM images of the epoxy nanocomposite with different contents of n-SiC particles are shown in Figure 2. The lower magnification images in Figure 2(a–c) give a general observation of n-SiC particles dispersion into the epoxy matrix. It can be seen that the n-SiC particles are homogeneously dispersed inside the epoxy matrix except for some particle agglomerations can be clearly seen at higher n-SiC loading. These agglomerations increase as n-SiC particle content increases. As it was observed during sample fabrication, the matrix viscosity significantly increased as nanoparticles concentration increased, which made particles dispersion rather poor and easily to aggregate in micro-size. At higher magnification images Figure 2(d–f), it can be seen that n-SiC particles have spherical shape with crystalline structure.

Mechanical properties

Flexural strength and modulus

Figures 3 and 4 illustrate the effect of n-SiC particles on the flexural strength and modulus of epoxy nanocomposites. Both flexural strength and modulus increase due the presence of n-SiC particles. In particular, flexural strength of epoxy increases by a maximum 21.5% with the addition of only 1% wt n-SiC. The enhancement in flexural strength may be ascribed to the good dispersion of n-SiC particles into the matrix, which increases matrix/n-SiC interaction surface providing good stress transferring from the matrix to the nanofillers resulting in an improve in sample strength properties. However, with further n-SiC loading (3 and 5%), flexural strength tends to decrease to values less than PE. The reason could be seen in Figure 2(a–c), at high concentration of n-SiC, n-SiC particles poorly dispersed inside the matrix forming particles agglomerations, which could weaken the adhesion strength between the matrix and the filler.[23,34] Besides, these agglomerations may act as stress concentrators, which in turn cause reduction in flexural strength.[23,25,34] Zainuddin et al.[25] investigated the flexural properties of epoxy/clay nanocomposites. Nanocomposites were fabricated with 1–3 wt % loading of montmorillonite layered silicate via magnetic stirring mixing for 5 h. Result showed that flexural strength was increased by a maximum up to 8.7% for samples reinforced with only 2 wt % of nanoclay compared to neat epoxy. Authors stated that poor dispersion of nanoclay led to poor mechanical properties.[25] Flexural modulus of epoxy nanocomposites are demonstrated in Figure 4. It can be seen that flexural modulus have similar trend to flexural strength values. The addition of (1, 3, and 5) wt % n-SiC significantly increase the modulus of epoxy system by 83, 59.2, and 58.9%, respectively. This expected result is due the fact that n-SiC particles have higher modulus than epoxy resin. Therefore, the presence of these rigid particles into the epoxy matrix increases the modulus of epoxy nanocomposites when compared with neat resin.[32]

The flexural strength of RCF reinforced n-SiC/epoxy nanocomposites are shown in Figure 3. It can be

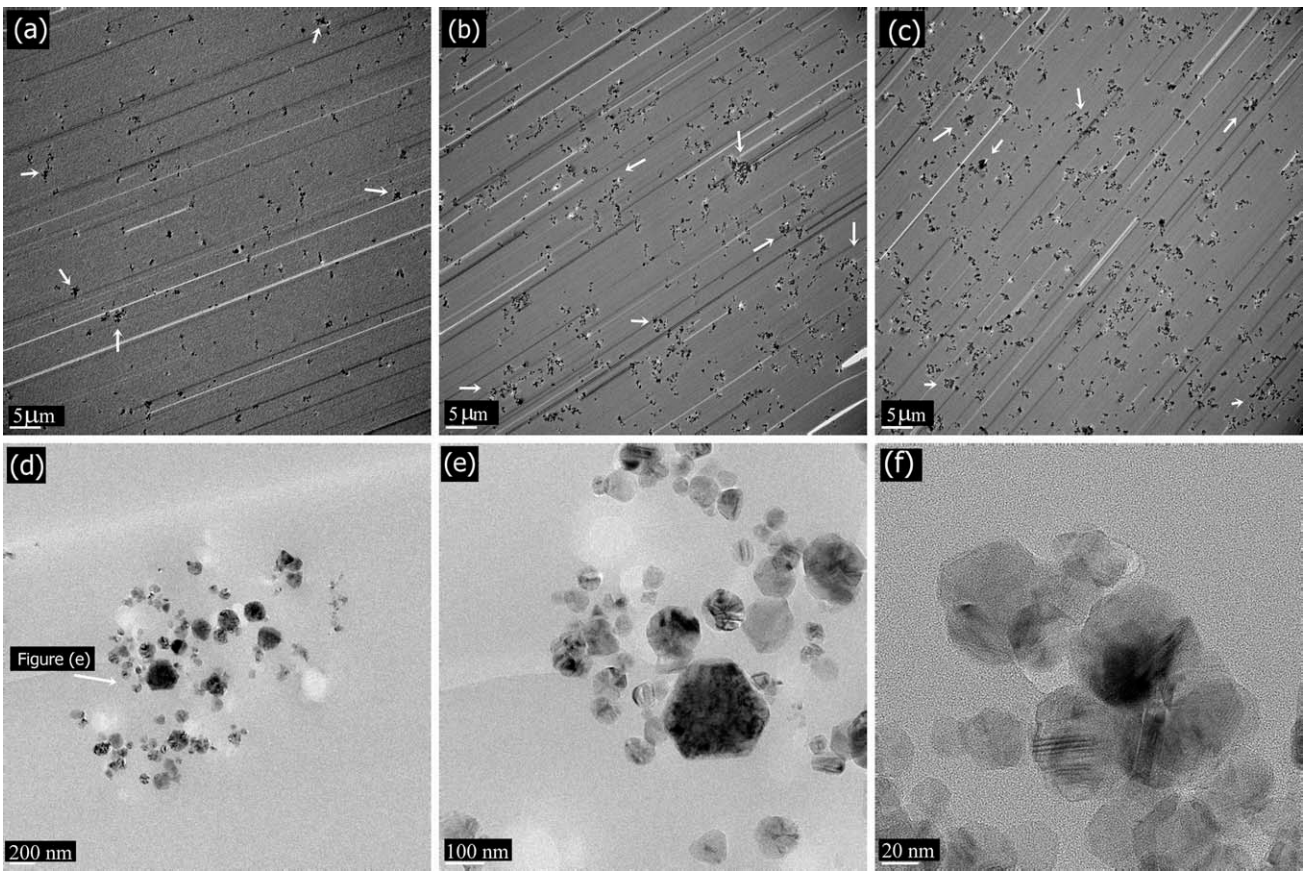

Figure 2 TEM micrographs of epoxy nanocomposites reinforced with different n-SiC concentration: (a) 1 wt %, (b) 3 wt %, (c) 5 wt %, and (d–f) are high magnification TEM images of n-SiC particles inside epoxy matrix. (The white arrows indicate n-SiC clusters).

seen that the presence of the RCF layers significantly improve the flexural strength for all kinds of samples. The flexural strength of the neat epoxy resin increase from 58.5 to 152.3 MPa after the addition of RCF layers with enhancement reaches up to 160%. This enhancement in flexural properties is due to the advantages of recycled cellulose fibers in resisting bending force of the composites.[26] In the case of RCF reinforced n-SiC/epoxy nanocomposites, the insertion of 1 wt % n-SiC slightly increases the flexural strength of RCF/epoxy composites. However, adding more SiC (3 and 5 wt %) lead to an insignificant reduction in strength. These results are in agreement with those obtained by Satapathy et al.[26] in their study on the influence of SiC particles derived from rice husk on flexural strength of jute/epoxy composites. Flexural strength was found insignificantly decreased after adding 10 and 20 wt % of SiC particles.[26] The presence of RCF into epoxy

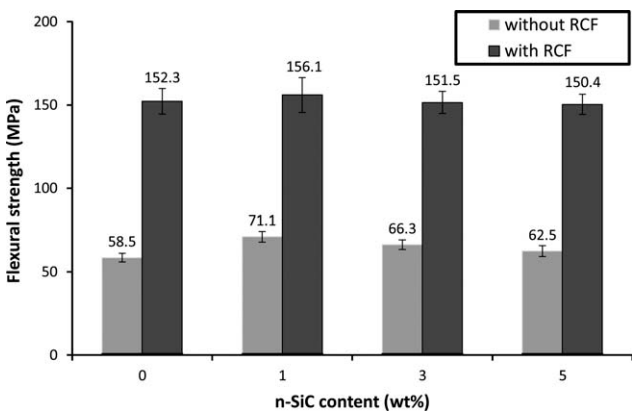

Figure 3 Flexural strength as a function of n-SiC content in unfilled composites and RCF-filled composites.

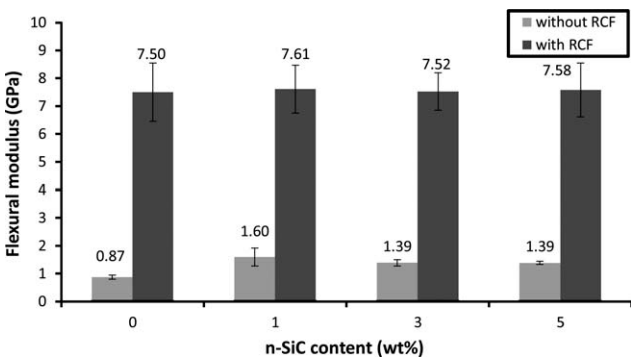

Figure 4 Flexural modulus as a function of n-SiC content in unfilled composites and RCF-filled composites.

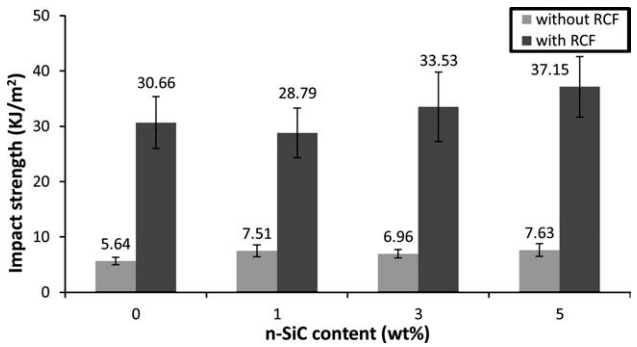

Figure 5 Impact strength as a function of n-SiC content in unfilled composites and RCF-filled composites.

matrix significantly increases the flexural modulus by about seven times compared to neat epoxy. Adding n-SiC particles to the RCF/epoxy slightly increases flexural modulus (Fig. 4).

Impact strength and toughness

The impact strength of epoxy nanocomposites and RCF reinforced epoxy nanocomposites are plotted in Figure 5. The presence of n-SiC particles increases the impact strength for epoxy nanocomposites with maximum improvement 35.5% at 5 wt % n-SiC load. The impact strength of neat epoxy increases from 5.6 to 7.5, 7.0, and 7.6 kJ/m^2 after the addition of 1, 3, and 5 wt % of n-SiC respectively. Similar significant enhancement in impact strength was reported by Lu et al.[35] They investigated the mechanical properties of hybrid epoxy/SiO_2 nanocomposites. It was found that impact strength for nanocomposites filled with 2 wt % SiO_2 increased by maximum 43.3% when compared with neat epoxy. However, adding more SiO_2 content (2.5 and 3) wt % caused impact strength to decrease due to the poor dispersion of SiO_2 particles at higher filler content. As illustrated in Figure 5, the presence of RCF significantly improves impact strength by $\sim$ 444% over PE from 5.6 to 30.7 kJ/m^2. This great achievement is due to the fact that cellulose fiber has a better ability to absorb impact energy than unreinforced polymer. This result is in agreement with the work of Maleque and Belal.[12] They studied the mechanical properties of pseudo-stem banana fiber-epoxy composites and found that the presence of banana woven fabric increased the impact strength over the neat epoxy by $\sim$ 40%. The effect of the addition of n-SiC on impact strength properties of RCF/epoxy nanocomposites is shown in Figure 5. It can be seen that impact strength of n-SiC filled RCF/epoxy nanocomposites increases as n-SiC loading increases. The impact strength of RCF/epoxy displays a maximum increase of 21% with only 5 wt % of n-SiC particles. It was observed an increase in n-SiC clusters into epoxy nanocomposites due to the increase in n-SiC loading as seen in Figure 2(a–c). These clusters may act as crack stoppers and increase the ability of the material to absorb energy by forming tortuous pathways for crack propagation, which resulting the impact strength to increase.[36]

The impact toughness in terms of the energy release rate (G_{1C}) for n-SiC/epoxy nanocomposites is illustrated in Figure 6. It can be seen that impact toughness gradually increases as the n-SiC content increases yielding a maximum at 5 wt % n-SiC load. The addition of 1, 3, and 5 wt % n-SiC into epoxy matrix significantly enhance impact toughness by 25.0, 50.0, and 62.5% over neat epoxy, respectively. This remarkable enhancement in toughness properties for nanocomposites is due to several toughness mechanisms for dissipating energy such as, crack pinning, crack deflection, particle debonding, plastic void growth, plastic deformation, and particle pullout as has been reported by number of studies for polymers reinforced with nanofillers.[29,30,32,37,38] Ma et al.[32] reported an increase in impact toughness of epoxy system due to the addition of nanofiller. Authors found that the inclusion of silica nanoparticles increased the toughness properties in terms of energy release rate (G_{1C}) of epoxy system by 81% at 20 wt % silica load. In the case of RCF/epoxy nanocomposites, the inclusion of RCF layers into epoxy resin remarkably enhances the impact toughness by about 262.5%. This extraordinary enhancement in toughness properties is due to the fact that RCF displays a variety of fracture mechanisms in the crack path to resist crack propagation.[11] These fracture mechanisms such as fiber breakage, fiber pullout, fiber debonding, and fiber bridging require high energy to be absorbed. The presence of n-SiC particles into RCF/epoxy increases impact toughness by 10.3, 24.1, and 27.6% at (1, 3, and 5) wt % n-SiC load, respectively. The extra improvement in impact toughness for RCF-based nanocomposites is due to the participating of n-SiC in resisting the crack growth.

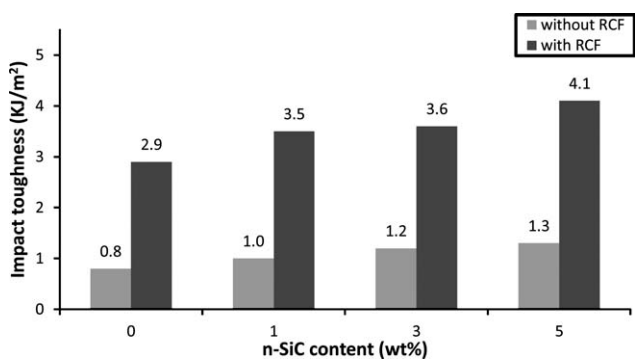

Figure 6 Impact toughness as a function of n-SiC content in unfilled composites and RCF-filled composites.

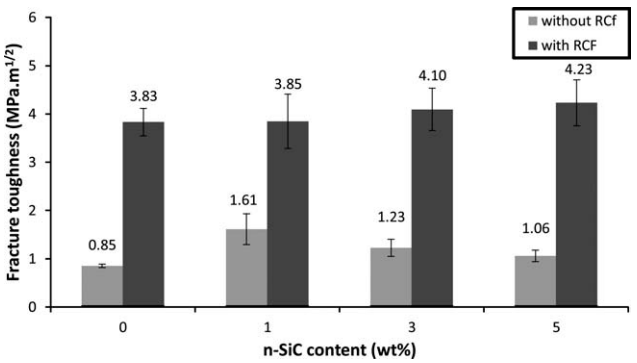

Figure 7 Fracture toughness as a function of n-SiC content in unfilled composites and RCF-filled composites.

Fracture toughness

The influence of n-SiC particles on fracture toughness of epoxy/n-SiC composites is shown in Figure 7. It can be seen that fracture toughness increases due to the presence of n-SiC particles. The addition of only 1 wt % n-SiC significantly increases facture toughness by a maximum 89.4% compared to neat epoxy. However, fracture toughness tends to decline as n-SiC content increases to (3 and 5) wt %. This could be due the poor dispersion of n-SiC and forming particle agglomeration at higher filler content as can be seen in Figure 2(a–c).[36,39] This significant enhancement in fracture toughness is similar to the work of Chen et al.[30] They found that the addition of (1 and 5) wt % of nanosilica to epoxy matrix increased fracture toughness by about 30%. However, adding more silica (10 wt %) led to decreasing in toughness.

The effect of RCF layers on fracture toughness is clearly shown in Figure 7. As expected, samples reinforced with RCF layers shows a significant increase in fracture toughness in all samples. For example, the addition of RCF in epoxy resin increased fracture toughness by about 350%. This extraordinary enhancement, as can be seen later in Figure 9, is due to the unique properties of cellulose fiber in resisting fracture, which resulted in increased energy dissipation from crack-deflection at the fiber–matrix interface, fiber debonding, fiber

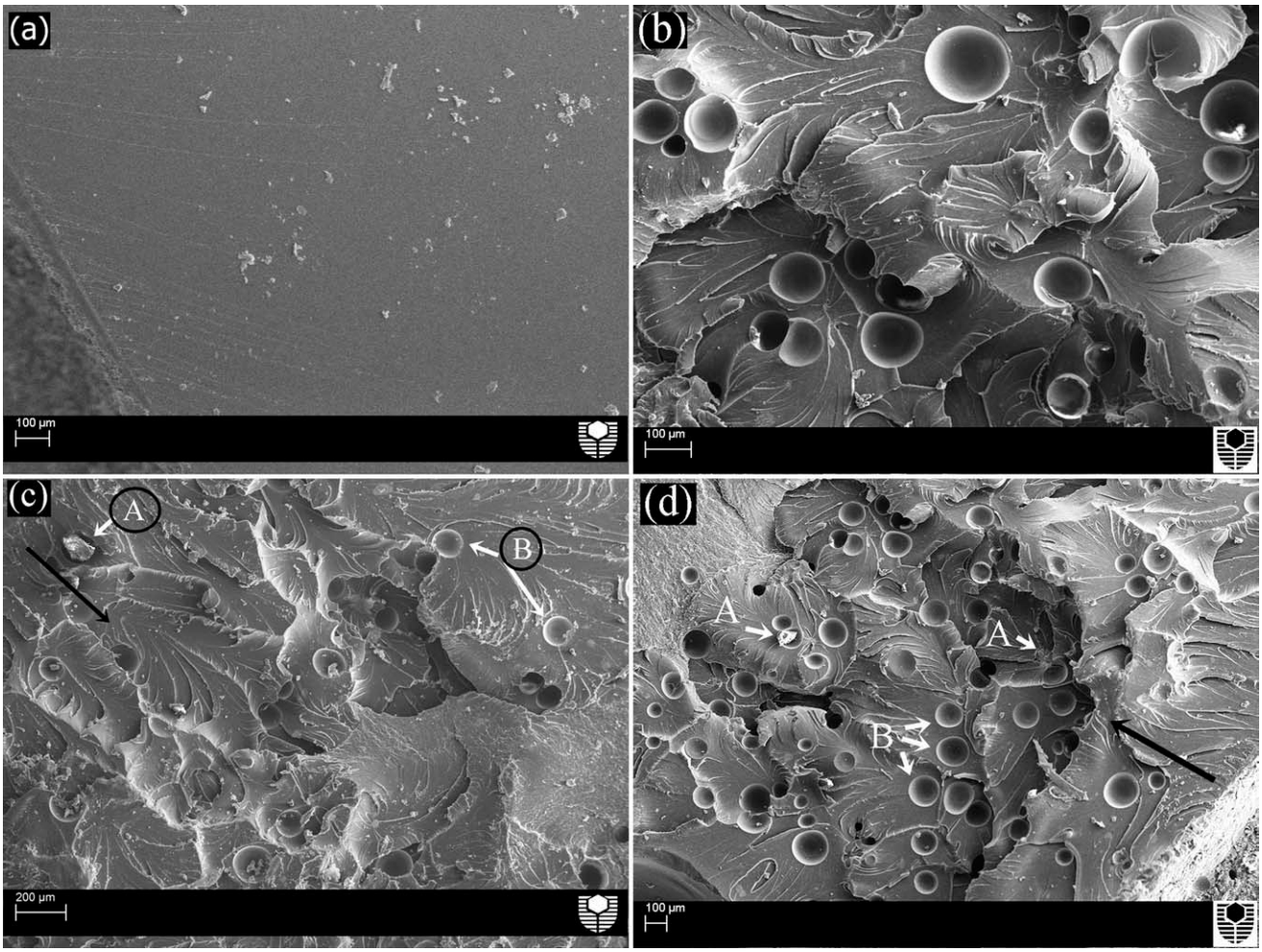

Figure 8 Scanning electron micrographs showing the fracture surfaces of: (a) PE, (b) PE/SiC5 (high magnification), (c) PE/SiC1, and (d) PE/SiC5. (Legend: (A) n-SiC clusters and (B) voids).

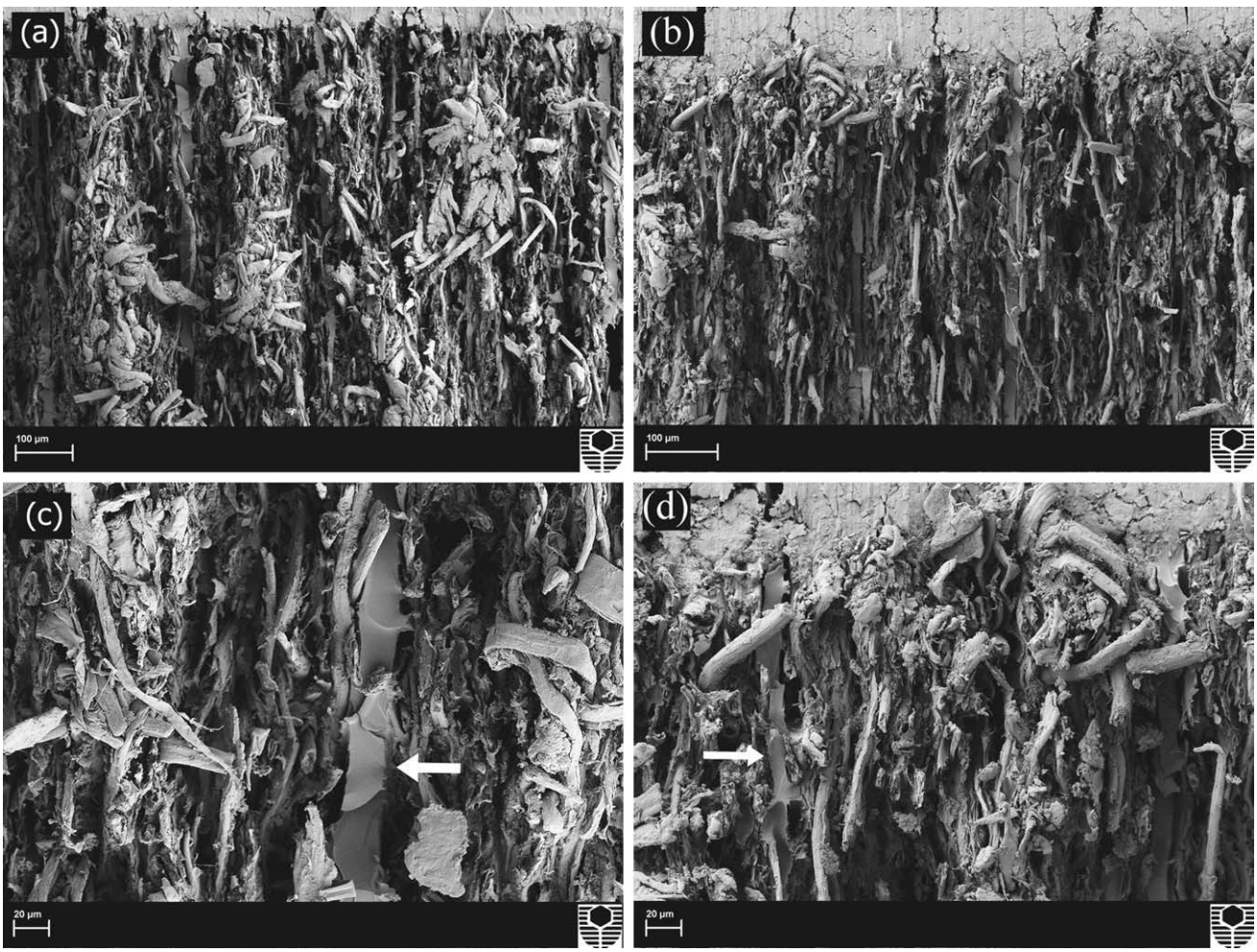

Figure 9 Scanning electron micrographs showing the fracture surfaces of: (a) PE/RCF, (b) PE/RCF/SiC1, (c) PE/RCF (high magnification), and (d) PE/RCF/SiC1 (high magnification). (The white arrow indicates the matrix).

bridging, fiber pullout, and fiber fracture.[11] This result is supported by the work of Lui and Huges[8] and Maleque and Belal.[12] They reported an enhancement in fracture toughness when cellulose fiber was added to epoxy matrix. In the case of epoxy eco-nanocomposites, the addition of n-SiC to the RCF/epoxy composites gradually increases the fracture toughness for all n-SiC filled RCF/epoxy samples. Fracture toughness of RCF/epoxy reinforced with 5 wt % n-SiC increases by maximum 10% over unfilled RCF/epoxy samples. This reveals that fracture toughness in RCF/epoxy eco-nanocomposites is mostly dominated by recycled cellulose fibers with slight effect of n-SiC particles.

Fracture surface and toughness mechanisms

The fracture surfaces of PE and epoxy nanocomposites reinforced with 1 and 5 wt % n-SiC particles are shown in Figure 8. It can be seen from Figure 8(a) that the fracture surface of PE is very smooth and featureless, which indicates typical brittle fracture behavior with lack of significant toughness mechanisms.[38] However, epoxy/n-SiC nanocomposites shows rougher fracture surfaces than that of neat resin as a result of the addition of nanofillers as can be seen in Figure 8(c,d). An increase in fracture surface roughness can be used as indicator to the presence of crack deflection mechanisms, which increase fracture toughness by increasing crack propagation length during deformation.[29,38] Figure 8(b) shows high magnification SEM micrograph of fracture surface for epoxy reinforced with 5 wt % n-SiC particles. A number of possible toughness mechanisms such as crack pinning, crack deflection, particle debonding, plastic void growth, plastic deformation, and particle pullout can be observed. Such toughness mechanisms can lead to higher fracture toughness properties through resisting crack propagation.[29,30,32,37,38] Moreover, particles agglomerations and voids in micro-scale are observed for epoxy/n-SiC nanocomposites. Samples with 5 wt % n-SiC shows increase in particle agglomerates and voids than samples filled with 1 wt % n-SiC. This result agrees with TEM results.

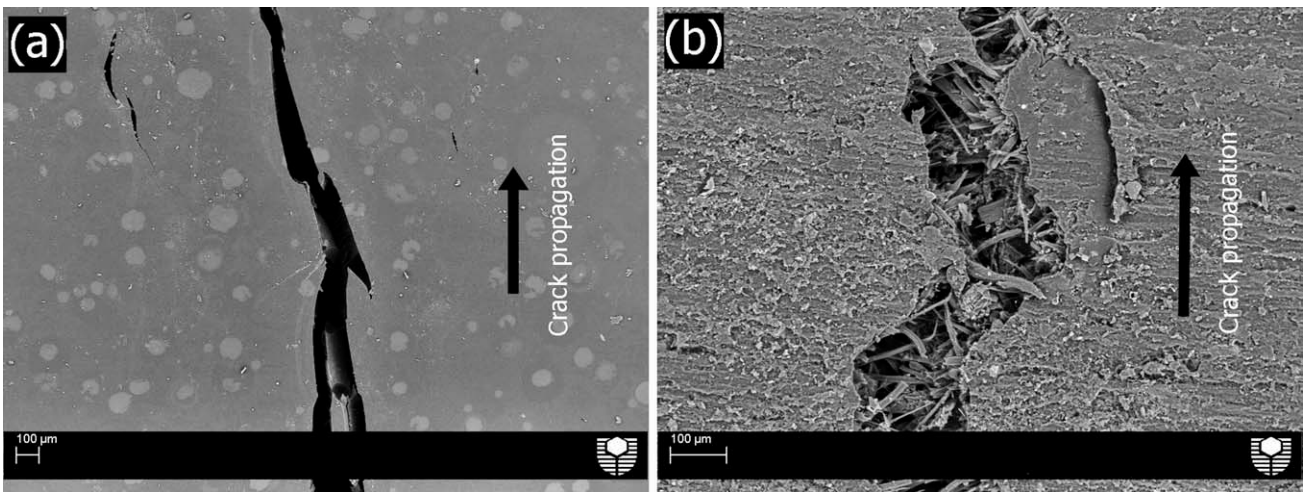

Figure 10 Scanning electron micrographs showing the crack propagation behavior in: (a) PE/SiC1 and (b) PE/RCF/SiC1.

Figure 9(a,b) illustrate low magnification image of RCF/epoxy sample and RCF/epoxy filled with 1 wt % n-SiC, while Figure 9(c,d) show high magnification image of same samples. A variety of toughness mechanisms such as, shear deformation, crack bridging, fiber pullout, and fiber fracture and matrix fracture can be clearly observed, which lead to good fracture properties of samples reinforced by RCF layers. Figure 10(a,b) display the back-scattered SEM images of crack propagation in epoxy/n-SiC and RCF/epoxy/n-SiC nanocomposites filled with 1% wt n-SiC. It is observed that samples reinforced with RCF layers did not completely break in two pieces. This is due to the fact that fibers bridge the cracks and enhance the crack propagation resistance, which lead to improvement in fracture toughness. The tortuous pathway for the crack propagations indicates the high energy absorbance by the RCF sheets. These super toughness mechanisms of RCF are the major factors of increasing mechanical properties of samples reinforced with RCF when compared with samples without RCF.

Thermal stability and properties

The thermal stability of the samples was determined using TGA. In this test, the thermal stability was studied in terms of the weight loss as a function of temperature in nitrogen atmosphere. The thermograms (TGA) and the derivatives thermograms (DTA) of neat epoxy, epoxy/RCF, epoxy/n-SiC, and epoxy/n-SiC/RCF nanocomposites filled with 5 wt % n-SiC are shown in Figures 11 and 12. The maximum decomposition temperature (T_{max}) and the char yields at different temperatures for all samples types are summarized in Table III.

In the case of epoxy resin and its nanocomposites, it can be seen from Table III that at low temperatures (<400°C) PE displays better thermal stability than those filled with n-SiC particles. This means that the presence of n-SiC accelerates the degradation of epoxy nanocomposites compared to epoxy

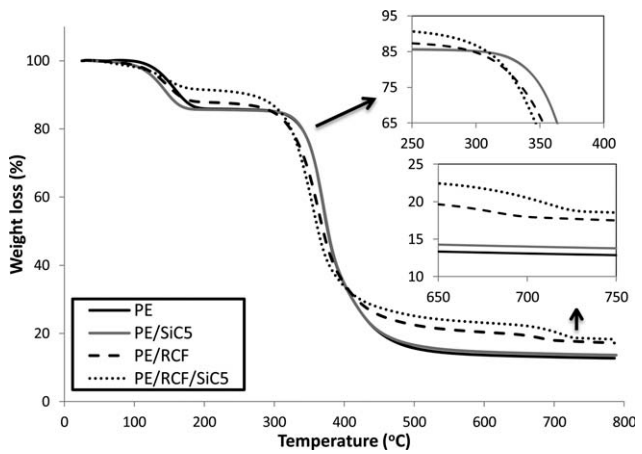

Figure 11 TGA curves of PE, PE/SiC5, PE/RCF, and PE/RCF/SiC5.

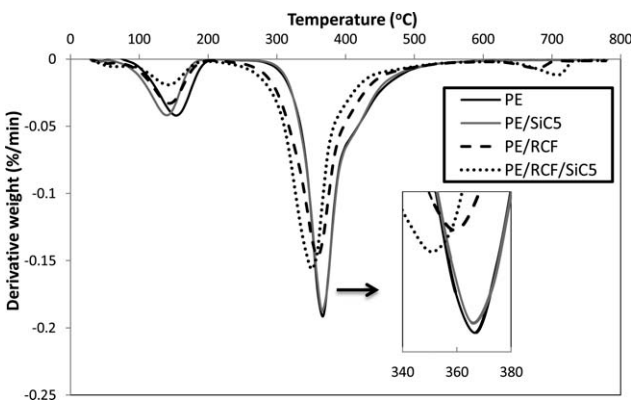

Figure 12 DTG curves of PE, PE/SiC5, PE/RCF, and PE/RCF/SiC5.

TABLE III
Thermal Properties of Epoxy, Epoxy/RCF Composites, Epoxy/n-SiC and Epoxy/RCF/n-SiC Nanocomposites

Sample	Char yield at different temperature (%)							T_{max} (°C)
	100°C	200°C	300°C	400°C	500°C	600°C	700°C	
PE	99.86	86.10	85.24	35.26	15.69	13.69	13.08	367.29
PE/SiC1	99.09	83.19	82.44	32.25	14.45	12.43	11.85	367.25
PE/SiC3	98.29	84.55	83.96	34.54	15.85	13.82	13.20	365.47
PE/SiC5	98.62	85.68	85.09	34.70	16.60	14.60	14.00	365.53
PE/RCF	98.65	87.88	85.01	34.58	22.49	20.37	17.96	359.62
PE/RCF/SiC1	97.34	94.30	88.48	33.72	26.90	25.15	21.66	351.43
PE/RCF/SiC3	97.96	92.74	87.65	33.83	25.84	23.92	20.87	351.37
PE/RCF/SiC5	98.22	91.51	86.65	33.84	25.15	23.14	20.50	350.87

resin. This observation has been reported as the Hofmann elimination reaction, where nanoparticles act as a catalyser toward the degradation of the polymer matrix.[40–42] The maximum decomposition temperature (T_{max}) of the nanocomposites slightly decreases by 2°C after the addition of (3 and 5) wt % n-SiC compared to PE. However, at high temperatures (>400°C), epoxy reinforced with 3 and 5 wt % n-SiC show better thermal stability than neat epoxy. The char residue at 700°C of neat epoxy increased from 13.1 to 13.2% and 14.0% after the addition of 3 and 5 wt % n-SiC, respectively. It was reported in previous studies that the addition of nanoparticles would efficiently raise the char residue of polymers at high temperature.[22,31,40,41]

The presence of RCF layers increases the amount of residue at temperatures range from 180 to 250°C. At the second decomposition where the major degradation occurs, the addition of RCF clearly decreases the maximum decomposition temperature (T_{max}) by 7.7°C compared to neat epoxy. Figure 12 shows that the peak of the maximum decomposition of RCF/epoxy composites shifted to lower temperature compared to neat epoxy, which indicates that the addition of RCF increases the rate of the sample major degradation. However, at high temperature (>400°C), where samples lose (>70%) of their initial weight, the presence of RCF leads to significant enhancement in thermal stability by increasing the char yield at 500, 600, and 700°C compared to epoxy system. The char yield at 700°C of neat epoxy increase from 13.1 to 18.0 wt % after the addition of RCF. Similar results were obtained by Shih[1] and De Rosa et al.[7] They reported an improvement in thermal stability of plant fiber/epoxy composites by increasing char yield at high temperatures. Shih[1] cited that the increasing in char yield is an indication of the potency of flame retardation of polymers. Thus, the addition of plant fiber enhanced the flame retardation of epoxy.

The addition of n-SiC to RCF/epoxy increases the thermal stability by increasing the amount of the residue at temperatures 200 and 300°C. However, at the region of major degradation, the unfilled RCF/epoxy shows better thermal stability than samples filled with n-SiC. The maximum decomposition temperature (T_{max}) of RCF/epoxy nanocomposites decreased by ~ 8°C compared to unfilled RCF/epoxy composite. Figure 12 shows that the peak of the major decomposition of RCF/epoxy filled with 5 wt % n-SiC moved to a lower temperature compared to unfilled RCF/epoxy composites. This is due to the catalytic effect of n-SiC particles on RCF/epoxy nanocomposites. But, at high temperatures (>400°C) n-SiC filled RCF/epoxy nanocomposites show better thermal stability than unfilled RCF/epoxy composite by increasing the char residues at temperatures 500, 600, and 700°C. This means that at high temperature, the addition of n-SiC particles significantly enhances the thermal stability of epoxy/RCF nanocomposites. This enhancement on thermal properties is due to the presence of n-SiC, which acted as barriers and hindered the diffusion of volatile decomposition products out from the nanocomposites.[40–43]

CONCLUSION

Epoxy ecocomposites and nanocomposites reinforced with recycled cellulose fibers (RCF) and n-SiC have been fabricated and characterized. The crystalline structure and the dispersion of the n-SiC particles into epoxy matrix were investigated by synchrotron radiation diffraction and TEM. The distribution of n-SiC particles was homogeneous with some particles agglomerations. In general, the inserting of n-SiC into epoxy matrix increased flexural strength, flexural modulus, impact strength, impact toughness and fracture toughness. The fracture surface features of modified epoxies were found to be rougher than neat epoxy due to the presence of n-SiC particles. The addition of n-SiC to epoxy matrix increased the thermal stability at high temperatures (above 400°C) when compared with neat epoxy.

The presence of RCF layers in the epoxy resin significantly increased all mechanical properties compared to neat epoxy and epoxy nanocomposites. This remarkable enhancement is due the unique

properties of cellulose fiber in withstanding bending force and resisting fracture force compared to brittle polymers. SEM micrographs showed a number of toughness mechanisms such as, shear deformation, crack bridging, fiber pullout and fiber fracture and matrix fracture. These super toughness mechanisms of RCF were the major factors of increasing mechanical properties of samples reinforced with RCF when compared with neat epoxy and its nanocomposites. The presence of RCF layers accelerated the major degradation for epoxy filled with RCF compared to neat epoxy. Maximum decomposition temperature decreased as a result to the addition of RCF layers.

The inclusion of n-SiC particles to the RCF/epoxy composites gradually increased fracture toughness and impact toughness compared to unfilled RCF/epoxy samples. Flexural strength increased after the addition of only 1 wt % n-SiC. However, adding more SiC caused decline in flexural strength due to the poor dispersion of n-SiC particles and formation of particle agglomerations at higher filler content. The addition of n-SiC to RCF/epoxy composites was found to increase the thermal stability by increasing the char yield of composites at high temperatures. However, the rate of degradation increased after adding n-SiC to RCF/epoxy composites by decreasing the maximum decomposition temperatures by about 8°C.

The authors thank Ms. E. Miller from Applied Physics at Curtin University of Technology for assistance with SEM, Dr. Rachid Sougrat from King Abdullah University of Science and Technology for performing the TEM images, Andreas Viereckl of Mechanical Engineering at Curtin University for the help with Charpy impact test, and Dr. Zied Alothman from King Saud University for assistance with TGA experiment. The collection of synchrotron powder diffraction data was funded by the Australian Synchrotron (PD-1654).

References

1. Shih, Y. F. Mater Sci Eng A 2007, 445, 289.
2. Deng, S.; Zhang, J.; Ye, L.; Wu, J. Polymer 2008, 49, 5119.
3. Ganan, P.; Garbizu, S.; Ponte, R.; Mondragon, I. Polym Compos 2005, 26, 121.
4. Dhakal, H. N.; Zhang, Z. Y.; Richardson, M. O. W. Compos Sci Technol 2007, 67, 1674.
5. Low, I. M.; McGrath, M.; Lawrence, D.; Schmidt, P.; Lane, J.; Latella, B. A. Compos A 2007, 38, 963.
6. Marsh, G. Mater Today 2003, 6, 36.
7. De Rosa, I. M.; Santulli, C.; Sarasini, F. Mater Design 2010, 31, 2397.
8. Lui, Q.; Hughes, M. Compos A 2008, 39, 1644.
9. Athijayamani, A.; Thiruchitrambalam, M.; Natarajan, U.; Pazhanivel, B. Mater Sci Eng A 2009, 517, 344.
10. Harish, S.; Michael, D. P.; Bensely, A.; Lal, D. M.; Rajadurai, A. Mater Character 2009, 60, 44.
11. Low, I. M.; Somers, J.; Kho, H. S.; Davies, I. J.; Latella, B. A. Compos Interface 2009, 16, 659.
12. Maleque, M. A.; Belal, F. Y. Arab J Sci Eng 2007, 32, 359.
13. Rashdi, A. A.; Sapuan, S. M.; Ahmad, M. M.; Khalina, A. J Food Agr Environ 2009, 7, 908.
14. Ma, J.; Xu, J.; Ren, J. H.; Yu, Z. Z.; Mai, Y. W. Polymer 2003, 44, 4619.
15. Lu, C.; Mai, Y. W. Phys Rev Lett 2005, 95, 088303.
16. Sinha, S. R.; Okamoto, M. Prog Polym Sci 2003, 28, 1539.
17. Usuki, A.; Kojima, Y.; Kawasumi, M.; Okada, A.; Fukushima, Y.; Kurauchi, T.; Kamigaito, O. J Mater Res 1993, 8, 1179.
18. Kojima, Y.; Usuki, A.; Kawasami, M.; Okada, A.; Fukushima, Y.; Karauchi, T.; Kamigaito, O. J Mater Res 1993, 8, 1185.
19. Alexandre, B.; Langevin, D.; Médéric, P.; Aubry, T.; Couderc, H.; Nguyen, Q. T.; Saiter, A.; Marais, S. J Membr Sci 2009, 328, 186.
20. Araujo, E. M.; Araujo, K. D.; Paz, R. A.; Gouveia, T. R.; Barbosa, R.; Ito, E. N. J Nanomaterials Vol. 2009, 2009, Article ID 136856, 5 pages.
21. Ha, S. R.; Rhee, K. Y.; Park, S. J.; Lee, J. H. Compos B 2010, 41, 602.
22. Hwang, S. S.; Liu, S. P.; Hsu, P. P.; Yeh, J. M.; Chang, K. C.; Lai, Y. Z. Int Commun Heat Mass Transfer 2010, 37, 1036.
23. Qi, B.; Zhang, Q. X.; Bannister, M.; Mai, Y. W. Compos Struct 2006, 75, 514.
24. Kaynak, C.; Nakas, G. I.; Lsitman, N. A. Appl Clay Sci 2009, 46, 319.
25. Zainuddin, S.; Hosura, M. V.; Zhoua, Y.; Narteha, A. T.; Kumarb, A.; Jeelani, S. Mater Sci Eng 2010, 527, 7920.
26. Satapathy, A.; Jha, A. k.; Mantry, S.; Singh, S. D.; Patnaik, A. J Reinforc Plast Compos 2010, 29, 2869.
27. Blackman, B. R. K.; Kinloch, A. J.; Sohn Lee, J., Talor, A. C.; Agarwal, R.; Schueneman, G. J Mater Sci 2007, 42, 7049.
28. Johnsen, B. B.; Kinloch, A. J.; Mohammed, R. D.; Taylor, A. C.; Sprenger, S. Polymer 2007, 48, 530.
29. Zhao, S.; Schadler, L. S.; Hillborg, H.; Auletta T. Compos Sci Technol 2008, 68, 2976.
30. Chen, C.; Justice, R. S.; Schaefer, D. W.; Baur, J. W. Polymer 2008, 49, 3805.
31. Chatterjee, A.; Islam, M. A. Mater Sci Eng A 2008, 487, 574.
32. Ma, J.; Mo, M. S.; Du, X. S.; Rosso, P.; Friedrich, K.; Kuan, H. C. Polymer 2008, 49, 3510.
33. Technical Information of Sigma-Aldrich. LLC. Available at http://www.sigmaaldrich.com/australia.html, 2011.
34. Xu, Y.; Hoa, S. V. Compos Sci Technol 2008, 68, 854.
35. Lu, S-R.; Jiang, Y-M.; Wei, C. J Mater Sci 2009, 44, 4047.
36. Deng, S.; Zhang, J.; Ye, L. Compos Sci Technol 2009, 69, 2497.
37. Wetzel, B.; Rosso, P.; Haupert, F.; Friedrich, K. Eng Fract Mech 2006, 73, 2375.
38. Tang, Y.; Deng, S.; Ye, L.; Yang, C.; Yuan, Q.; Zhang, J.; Zhao, C. Compos A 2011, 42, 345.
39. Yasmin, A.; Abot, J. L.; Daniel, I. M. Script Mater 2003, 49, 81.
40. Madaleno, L.; Schjødt-Thomsen, J.; Pinto, J. C. Compos Sci Technol 2010, 70, 804.
41. Ismail, H.; Pasbakhsh, P.; Fauzi, M. N. A.; Abu Bakar, A. Polym Test 2008, 27, 841.
42. Zhao, C.; Qin, H.; Gong, F.; Feng, M.; Zhang, S.; Yang, M. Polym Degrad Stab 2005, 87, 183.
43. Yeh, J. M.; Huang, H. Y.; Chena, C. L.; Su, W. F.; Yu, Y. H. Surf Coat Technol 2006, 200, 2753.